Medicine®

OPEN

Diagnostic agreement between 3.0-T MRI sequences of nerve root and surgery in patients with cervical radiculopathy
A retrospective study

Qi Wang, BS[a], Huixia Li, MS[a], Jianjun Kong, BS[b], Xiaohui Li, BS[a], Lin Feng, BS[a], Zhanyong Wu, MS[b,*] ⓘD

Abstract

Currently, minute structures, such as cervical nerve roots, can be viewed using magnetic resonance imaging (MRI) sequences; however, studies comparing multiple sequences in the same set of patients are rare. The aim of the study is to compare the diagnostic values of three 3.0-T MRI sequences used in the imaging of cervical nerve roots.

This study included 2 phases. In the first phase (n = 45 patients), the most optimal MRI sequence was determined. In the second phase, this MRI sequence was compared with surgical results (n = 31 patients). The three-dimensional double-echo steady-state (3D-DESS), multi-echo data image combination (MEDIC), and 3D sampling perfection with application-optimized contrasts using different flip angle evolutions (3D-SPACE) sequences were performed to analyze the image quality. Furthermore, the most optimal MRI sequence was compared with surgical results to determine the agreement rate.

The image quality scores of the 3 sequences were significantly different ($P < .05$). The score for 3D-DESS sequence was superior to that of MEDIC sequence, while the score for 3D-SPACE sequence was the worst. For visualization of compressed nerve roots, 3D-DESS sequence was superior to the other 2 sequences in terms of the total quality score and compressed nerve root score. Therefore, 3D-DESS sequence was used for MRI in 31 patients with cervical spondylosis in the second phase of this study. The diagnostic agreement rate was 93.5%.

This study concluded that in patients with cervical radiculopathy, the 3D-DESS sequence is superior to the MEDIC and 3D-SPACE sequences and shows a high agreement rate with the surgical diagnosis.

Abbreviations: 3D-DESS = three-dimensional double-echo steady-state, 3D-SPACE = 3D sampling perfection with application-optimized contrasts using different flip angle evolutions, CNR = contrast-to-noise ratio, CPR = curved planar reformation, FOV = field of vision, ICC = intra-class correlation coefficient, MEDIC = multi-echo data image combination, MIP = maximum intensity projection, MPR = multi-planar reformation, MRI = magnetic resonance imaging, SAG = sagittal plane, T1WI = T1-weighted imaging, T2WI = T2-weighted imaging, TE = echo time, TR = repetition time, TRA = transversal, TSE = turbo spin echo.

Keywords: agreement, magnetic resonance imaging, radiculopathy, sequences, surgery

1. Introduction

Cervical radicular pain occurs due to impingement of cervical nerves and/or nerve roots. It is typically characterized by unilateral shooting electric pain in the upper limb and neck pain. In patients with radiculopathy, the pain results from sensory, motor, and/or reflex deficits.[1–3] The reported annual incidence of cervical radiculopathy is about 83 per 100,000 persons.[4] The underlying pathology of cervical radiculopathy is usually of degenerative nature.[1] The symptoms from cervical vertebral lesions often include the clinical symptoms of cervical nerve root injury.[5]

In recent years, minimally invasive surgery, such as keyhole decompression under the posterior cervical dilatation channel, has been favored over open surgery for the treatment of cervical spondylotic radiculopathy because of smaller trauma and good outcomes.[6] The indications for the minimally invasive procedure are confirmation of the presence of a lesion during imaging, presence of symptoms for more than 6 months, compression ratio < 0.4, and failure in using conservative treatments.[7–9] This procedure is carried out through the decompression of intervertebral foramen and removal of nucleus pulposus under direct visualization of the channel.[6] The procedure follows an interstitial approach through the paraspinal muscles, and the surgical field is small, requiring high precision. Therefore, clear

visualization of the shape and movement of the nerve roots before surgery is of great clinical significance.

Cervical magnetic resonance imaging (MRI) can easily show structural changes in the intervertebral disc, spinal canal, and spinal cord; however, the anatomy of the cervical nerve roots is complex, and their shape is slender. Therefore, a conventional MRI examination shows poor resolution for nerve roots.[10,11] Early studies showed that contrast-enhanced MRI used for the imaging of cervical nerve roots has certain advantages,[12,13] but it involves the injection of the contrast agent Gd-DTPA before scanning, which is associated with complications in some patients.[14,15]

In recent years, with the development of MRI equipment and technology, research related to spinal nerve root imaging has been blooming. Novel MRI sequences, such as three-dimensional double-echo steady-state (3D-DESS), multi-echo data image combination (MEDIC), and 3D sampling perfection with application-optimized contrasts using different flip angle evolutions (3D-SPACE), have been found to be of value for the imaging of larger lumbosacral nerve roots.[16–20] Compared with regular sequences, all of these aim to avoid the traditional compromises in signal-to-noise ratio, spatial resolution, and contrast resolution; hence, in these MRI sequences, the sensitivity and specificity has increased and the increased resolution allows viewing of minute structures.[16–20] Studies comparing multiple MRI sequences in the same set of patients are rare. Selection of the most appropriate scanning sequence during MRI and clear and effective imaging of the cervical nerve root structure is particularly important.

Therefore, the aim of this study was to compare the characteristics of the 3D-DESS, MEDIC, and 3D-SPACE sequences used for cervical nerve root imaging, evaluate the application value of the 3 sequences in cervical nerve root imaging, determine the most optimal nerve root imaging sequence, and compare the imaging-based diagnosis with the surgical diagnosis.

2. Materials and methods

2.1. Study design and patients

This study comprises 2 phases. In the first phase, the most optimal MRI sequence was determined. In the second phase, this sequence was compared with surgical results.

In the first phase, 45 consecutive patients who underwent cervical MRI at the Spinal Surgery Department of our hospital between July 2017 and March 2018 were included. This study complies with the ethical standards of the relevant national guidelines on human experimentation and the Helsinki Declaration of 1975, as revised in 2008. This study has been approved by the institutional committee of Jizhong Energy Xingtai Mining Group General Hospital. The consents were obtained from the patients included in this study.

The inclusion criteria were:

1) patients whose physical examination results were normal but required cervical MRI because of a clinical diagnosis of cervical spondylosis and
2) ≥18 years of age.

In this study, cervical spondylosis was clinically diagnosed using patient's medical history and physical examination findings of unilateral shooting electric pain in the upper limb, neck pain, and pain due to sensory, motor, and/or reflex deficits; provocative tests may also help in the diagnosis.[1–3]

The exclusion criteria were:

1) cervical deformity;
2) history of cervical spine surgery;
3) contraindications of MRI (e.g., patients with claustrophobia, cardiac pacemakers, or metal implants or pregnant patients); or
4) acute trauma and motion artifacts due to the inability to resist pain during the scan, which may affect the nerve root imaging.

2.2. MRI

MRI was performed using a 3.0-T Skyra magnetic resonance imager (Siemens, Erlangen, Germany), spine matrix coil, and a special coil for neck scanning. The patients were required to be in the supine position, with calm breathing, head advanced, and the cervical vertebrae in the normal position. The conventional cervical MRI sequences (sagittal axis T1-weighted imaging [T1WI], sagittal axis T2-weighted imaging [T2WI], and horizontal axis T2WI) were performed, followed by the MEDIC, 3D-SPACE, and 3D-DESS sequences. The 3 scanning sequences and parameters are shown in Table 1. For patients in the second phase of this study, MRI was performed within 3 days prior to surgery.

2.3. Data processing

The raw data of MRI were transferred to the Siemens 3D Post-Processing System (SYNGO) for post-processing reconstruction, including maximum intensity projection (MIP), multi-planar reformation (MPR), and curved planar reformation (CPR). The layer thickness and spacing of the 3 post-process sequences were consistent.

Table 1

MRI sequence parameters.

Sequence	TR (ms)	TE (ms)	FOV (mm)	Acquisition times	Flip angle (°)	Layer thickness (mm)	Spacing (mm)	Pitch	Matrix bandwidth (Hz/Px)	Scan time (min)
T1WI/SAG	936	9	260	1	150	3.5	0.7	224 × 320	260	1:15
T2WI/SAG	3670	112	260	1	160	3.5	0.7	224 × 320	260	1:24
T2WI/TRA	2900	107	200	2	160	3.0	0.3	224 × 320	284	2:38
3D-DESS	14	5	280	1	25	0.7	0.2	256 × 256	395	3:31
MEDIC	22	12	280	1	20	1.5	0.8	240 × 320	252	6:22
3D-SPACE	3500	3500	250	1	150	1.0	0.0	243 × 256	630	4:59

3D-DESS = three-dimensional double-echo steady-state, 3D-SPACE = 3D sampling perfection with application-optimized contrasts using different flip angle evolutions, FOV = field of vision, MEDIC = multi-echo data image combination, MRI = magnetic resonance imaging, SAG = sagittal plane, T1WI = T1-weighted imaging, T2WI = T2-weighted imaging, TE = echo time, TR = repetition time, TRA = transversal.

Table 2

Contrast-to-noise ratio and image quality scores of the 3D-DESS, MEDIC, and 3D-SPACE sequences.

Sequence	Nerve root-vertebral CNR	Nerve root-cerebrospinal fluid CNR	Image quality score				Total score	Compressed cervical nerve clarity score
			1	2	3	4		
3D-DESS	133.4 ± 91.4	119.7 ± 78.6	2.8 ± 0.4	2.9 ± 0.3	2.7 ± 0.5	2.6 ± 0.5	11.0 ± 1.2	2.7 ± 0.5
MEDIC	62.7 ± 56.3	26.7 ± 27.2	2.1 ± 0.5	2.3 ± 0.8	2.0 ± 0.6	1.9 ± 0.6	8.3 ± 1.9	2.2 ± 0.7
3D-SPACE	77.8 ± 96.4	170.0 ± 125.2	1.5 ± 0.8	1.4 ± 0.9	1.2 ± 0.7	1.2 ± 0.7	5.2 ± 2.8	1.3 ± 0.6

All data are shown as means ± standard deviations. Item 1: whether the image was clear. Item 2: whether the morphology of the normal nerve root was continuous. Item 3: whether the normal nerve root boundary was clear. Item 4: whether the normal nerve root edge was smooth and sharp. 3D-DESS = three-dimensional double-echo steady-state, 3D-SPACE = 3D sampling perfection with application-optimized contrasts using different flip angle evolutions, CNR = contrast-to-noise ratio, MEDIC = multi-echo data image combination.

2.4. Image evaluation

Measurements and evaluations were performed independently by 2 senior diagnostic radiologists with more than 5 years of experience. The contrast-to-noise ratio (CNR) of the cervical nerve root and adjacent tissue was measured at the workstation. Image quality and imaging of the normal cervical nerve root and compression of the cervical nerve were graded, and the results were finally averaged.[21,22] For each sequence, the image quality score was determined considering the following 4 aspects: whether the image was clear; whether the morphology of the normal nerve root was continuous; whether the normal nerve root boundary was clear; and whether the normal nerve root edge was smooth and sharp. Each item was graded as good, fair, and poor, which were represented by 3, 2, and 1 points, respectively. The quality of the visualization of the compressed cervical nerve was graded as clear, lack of good quality, and unclear, which were represented by 3, 2, and 1 points, respectively.

2.5. Agreement between MRI and surgical diagnoses of radiculopathy

In the second phase of the study, the optimal sequence scan was performed in 31 patients with cervical spondylotic radiculopathy. The inclusion and exclusion criteria were the same as for the first phase of the study. The results of the imaging diagnosis were compared with those of the surgical diagnosis of radiculopathy. The agreement rate was calculated as the number of cases of diagnostic match/total number of cases × 100%.

2.6. Statistical analysis

All data were analyzed using SPSS 23.0 (IBM, Armonk, NY). The consistency of the scores between the 2 readers was evaluated using the intra-class correlation coefficient (ICC). Continuous data were tested using the Kolmogorov–Smirnov test for normal distribution and were presented as mean ± standard deviation and analyzed using the ANOVA (normal distribution), or medians (ranges), and the rank sum test (skewed distribution). Categorical data were presented as numbers and percentages and analyzed using Fisher's exact test. Two-sided P-values <.05 were considered statistically significant.

3. Results

3.1. Characteristics of patients

In this study, 21 men and 24 women aged 48.0 ± 11.2 (range, 24–67) years were included. The clinical course of cervical radiculopathy was 2 months to 15 years.

3.2. Selection of the most optimal MRI sequence

The ICC evaluation of the scores between the 2 readers showed that they were consistent ($r = 0.962$). The results of the 3 types of MRI sequences and data measurement are shown in Table 2. The comparison of the 3 MRI sequences is shown in Table 3. The comparisons of the 3 sequences show that they differ significantly in terms of image quality. Figure 1 presents a typical case.

CNR of nerve root-vertebrae and CNR of nerve root-cerebrospinal fluid with the 3D-DESS sequence were higher than that in the MEDIC sequence ($P < .05$). The CNR of nerve root-vertebrae in the 3D-DESS sequence was higher than that in the 3D-SPACE sequence ($P < .05$), while the CNR of nerve root-cerebrospinal fluid with the 3D-DESS sequence was lower than that with the 3D-SPACE sequence ($P < .05$). The CNR of nerve root-cerebrospinal fluid with the 3D-SPACE sequence was higher than that with the MEDIC sequence ($P < .05$). No significant difference was observed between the CNR of nerve root-vertebrae in the 3D-SPACE and MEDIC sequences.

Table 3

Comparison of the 3D-DESS, MEDIC, and 3D-SPACE sequences.

Comparison	Nerve root-vertebral CNR	Nerve root-cerebrospinal fluid CNR	Image quality score				Total score	Compressed cervical nerve clarity score
			1	2	3	4		
3D-DESS vs MEDIC	<0.001	<0.001	<0.001	0.001	<0.001	0.001	<0.001	0.013
3D-DESS vs 3D-SPACE	0.002	0.007	<0.001	<0.001	<0.001	<0.001	<0.001	<0.001
MEDIC vs 3D-SPACE	0.390	<0.001	<0.001	<0.001	<0.001	<0.001	<0.001	<0.001

All data are shown as P-values. Item 1: whether the image was clear. Item 2: whether the morphology of the normal nerve root was continuous. Item 3: whether the normal nerve root boundary was clear. Item 4: whether the normal nerve root edge was smooth and sharp. 3D-DESS = three-dimensional double-echo steady-state, 3D-SPACE = 3D sampling perfection with application-optimized contrasts using different flip angle evolutions, CNR = contrast-to-noise ratio, MEDIC = multi-echo data image combination.
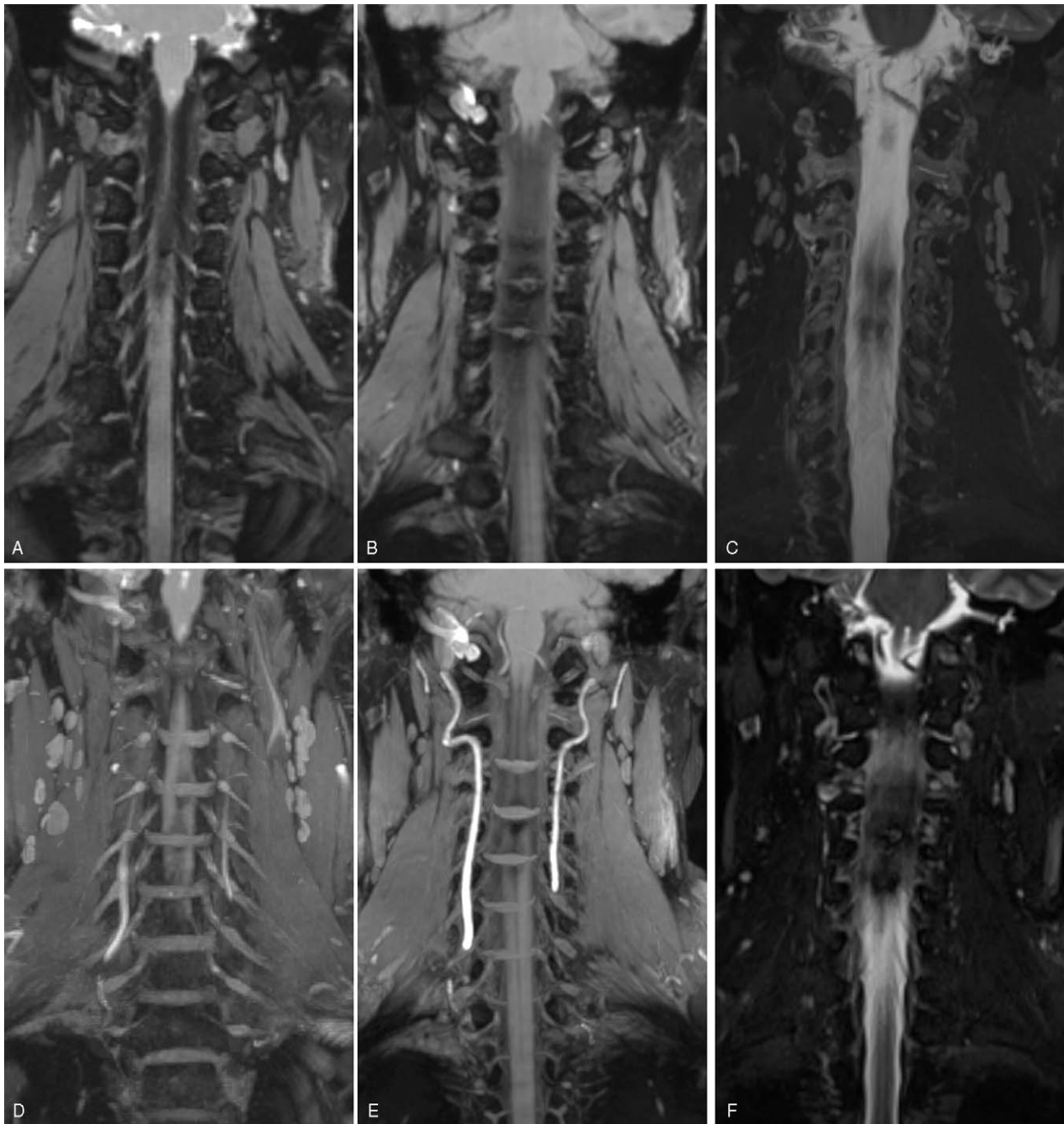
Figure 1. A typical case of a 38-year-old female with neck pain for 3 mo. Thin-layer reconstruction of coronal image from the (A) 3D-DESS, (B) MEDIC, and (C) 3D-SPACE sequences. Thick-layer reconstruction of the coronal image from the (D) 3D-DESS, (E) MEDIC, and (F) 3D-SPACE sequences. The image clarity of the 3D-DESS sequence was better than that of the other 2 sequences, and the contrast between the nerve and the surrounding tissue was higher as well.

The image quality scores of the 3 sequences were significantly different (all $P < .05$). The image quality of the 3D-DESS sequence was superior to that of the MEDIC sequence, while the 3D-SPACE sequence had the worst image quality. For the visualization of compressed nerve roots, the 3 sequences showed significantly different findings ($P < .05$). The 3D-DESS sequence was found to be superior to the MEDIC and 3D-SPACE sequences in terms of visualization of compressed nerve roots.

3.3. Agreement between MRI and surgery

The diagnostic results of 3D-DESS sequence in 31 patients with cervical spondylosis were compared with that of surgical diagnosis. The diagnostic agreement rate was 93.5%. A typical case is shown in Figure 2. The imaging diagnosis was not in agreement with the surgical diagnosis in 2 patients. One patient had hyperplasia of the peripheral facet joints and the compressed nerve roots were poorly displayed; therefore, no precise diagnosis could be obtained. The other patient had evident clinical
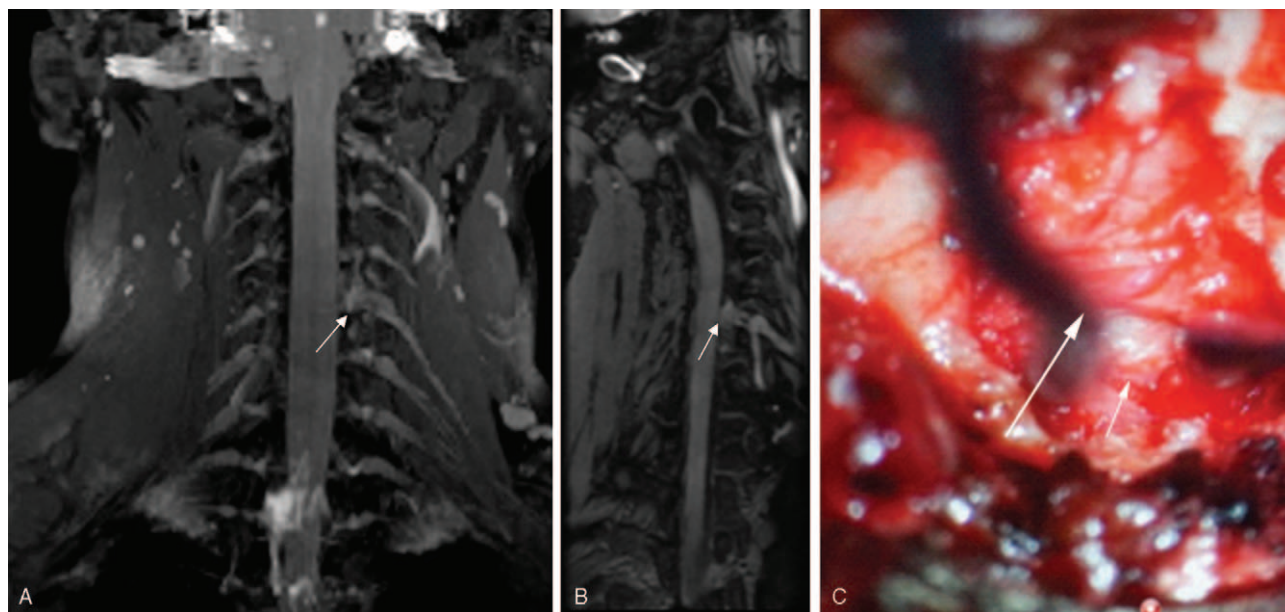
Figure 2. A typical case of a 44-year-old female with numbness and weakness in the left upper limb for 10 d. Physical examinations showed that the range of motion of the cervical vertebrae was good, while pressing pain in the posterior cervix was found. The muscle strength of the left upper limb was Grade 1. (A and B) Reconstructed coronal and oblique sagittal images of the 3D-DESS sequence, which show the left-posterior protrusion of the C5–C6 intervertebral disc, as well as the oppression of the left nerve root (white arrows). (C) Surgical findings, which show the oppression of the nerve root (long arrow) by the intervertebral disc (short arrow).

symptoms. The intraoperative findings showed that the nerve roots were thickened and red. However, no evident oppressive changes were found. These findings suggested that the 3D-DESS sequence could allow precise diagnosis of nerve root compression in most of the cases. Nevertheless, 3D-DESS sequence could have diagnostic limitations for bone hyperplasia or calcification.

4. Discussion

Various studies state that novel MRI sequences allow viewing of minute structures, such as cervical nerve roots[16–20]; however, studies comparing multiple sequences in the same set of patients are limited. Therefore, this study aimed to compare the diagnostic value of three 3.0-T MRI sequences in the imaging of cervical nerve roots. The results suggest that in patients with cervical radiculopathy, the 3D-DESS sequence is superior to the MEDIC and 3D-SPACE sequences and shows a high agreement rate with the surgical diagnosis.

The 3D-SPACE sequence uses hard pulses as the reverberation pulse with a short echo interval, variable excitation angle, and large signal area to collect more data at the same time, realizing fast and high-resolution 3D turbo spin echo (TSE) contrast imaging with high CNR for lesion boundaries and surrounding tissue structures.[17,20,23] Studies have shown that the 3D-SPACE sequences have certain advantages in the comprehensive evaluation of lumbar lesions[23]; however, limited research has been conducted regarding cervical radiculopathy. The results of this study showed that the CNR of nerve root and cerebrospinal fluid with 3D-SPACE sequence was relatively higher; however, the image quality score with 3D-SPACE sequence was lower than that of 3D-DESS and MEDIC sequences. The 3D-SPACE sequence adopts short tau inversion recovery technique combined with chemical shift fat suppression technology to yield a good and uniform fat suppression effect and relatively better

signal intensity and contrast of the peripheral nerve.[17,20,23] In the high-signal cerebrospinal fluid, the contrast of the low-signal intervertebral disc is particularly more obvious. Therefore, the CNR of nerve root and cerebrospinal fluid with 3D-SPACE sequence was higher than that of the 3D-DESS and MEDIC sequences. However, still the 3D-SPACE sequence is not as good as the 3D-DESS and MEDIC sequences for the visualization of the cervical nerve root, especially for visualizing local small lesions of the compressed nerve root, and the clarity of the image is poor as well.

The MEDIC sequence[24] is a multi-gradient echo sequence acquired in the same phase-encoding after a small angle pulse excitation. It is characterized by the coincidence of multiple echo data images, and a water-stimulated sequence for a thin-layer high-resolution imaging with high isotropic resolution. In this study, the scores of image quality and visualization of the compressed nerve root with the MEDIC sequence were lower than that with the 3D-DESS sequence, indicating that the MEDIC sequence has certain advantages in visualizing local radiculopathy, but a disadvantage, which may be related to the low signal-to-noise ratio of the MEDIC sequence, is still present.

The 3D-DESS sequence captures T1WI, T2WI, and heavily T2WI effects in repetition time (TR), and these effects can be combined with fat suppression to form a fused image,[25] which can highlight long T2 liquid signals and anatomical details. It is less affected by capillaries and is not sensitive to respiratory movement. Using MIP and CPR, 3D-DESS neuroimaging can yield detailed images of the coronal surface when the signal is collected. Therefore, the full length of the nerve root in the cervical nerve can be visualized on the same level as much as possible, thereby clearly showing the anatomical position of the nerve root and surrounding tissue and clarifying the existence and specific location of the nerve root compression. The 3D-DESS sequence is already known to be of value for radiculopathy.[18,25]

The present study showed that the image quality and the clarity score for the visualization of the compressed nerve root with the 3D-DESS sequence were higher than that in the MEDIC and 3D-SPACE sequences. The contrast signal-to-noise ratio in the 3D-DESS sequence was observed to be significantly higher than that in the MEDIC sequence. Additionally, the scan time was the shortest with the 3D-DESS sequence among the 3 sequences. Therefore, the 3D-DESS sequence was found to be superior to the MEDIC and 3D-SPACE sequences in terms of image contrast signal-to-noise ratio and overall image quality.

In the second phase of this study, the results of the 3D-DESS sequence imaging diagnosis in 31 patients with cervical spondylosis were compared with the findings obtained in surgical diagnosis. The diagnostic agreement rate was 93.5%, and 2 cases did not show consistency between the imaging and surgical findings. In 1 patient, hyperplasia of the peripheral facet joints obscured the nerve roots and did not allow a precise diagnosis. The other patient had obvious clinical symptoms and inflamed nerve root, but no cause could be identified. Therefore, additional studies are necessary to determine the factors that could lead to misdiagnosis in radiculopathy using the 3D-DESS sequence.

This study has few limitations. The sample size was small and data were collected from a single center. Based on data availability, we used 2 groups of patients, which could introduce bias. Moreover, we compared the imaging diagnosis of the 3D-DESS sequence only with the surgical diagnosis. Therefore, we could not examine the agreement of all of the 3 sequences with the surgery results. Future studies with larger sample, comparing the imaging diagnosis of each sequence with the surgical diagnosis will be required to address these limitations.

In conclusion, the 3D-DESS sequence is relatively more comprehensive and more practical in visualizing the nerve root structure and local lesions of the compressed nerve root in patients with cervical radiculopathy. This technique also shows a high agreement rate with the surgical diagnosis. Therefore, this study states that the 3D-DESS sequence could provide a reliable reference for early and accurate diagnosis of cervical nerve root compression.

Acknowledgments

Author contributions

Conceptualization: Qi Wang.
Data curation: Qi Wang, Zhanyong Wu.
Formal analysis: Qi Wang, Xiaohui Li, Zhanyong Wu.
Investigation: Jianjun Kong.
Methodology: Huixia Li, Lin Feng.
Project administration: Jianjun Kong.
Supervision: Huixia Li, Xiaohui Li.
Validation: Jianjun Kong, Lin Feng.
Writing – original draft: Qi Wang.
Writing – review & editing: Qi Wang, Zhanyong Wu.

References

[1] Childress MA, Becker BA. Nonoperative management of cervical radiculopathy. Am Fam Physician 2016;93:746–54.

[2] Bono CM, Ghiselli G, Gilbert TJ, et al. An evidence-based clinical guideline for the diagnosis and treatment of cervical radiculopathy from degenerative disorders. Spine J 2011;11:64–72.

[3] Van Zundert J, Huntoon M, Patijn J, et al. 4. Cervical radicular pain. Pain Pract 2010;10:1–7.

[4] Radhakrishnan K, Litchy WJ, O'Fallon WM, et al. Epidemiology of cervical radiculopathy. A population-based study from Rochester, Minnesota, 1976 through 1990. Brain 1994;117(Pt 2):325–35.

[5] Corey DL, Comeau D. Cervical radiculopathy. Med Clin North Am 2014;98:791–9. xii.

[6] Wu Z, Wu H, Wang H, et al. A rare complication after minimally invasive posterior cervical laminoforaminotomy. J Musculoskelet Neuronal Interact 2016;16:172–3.

[7] Hur JW, Kim JS, Shin MH, et al. Minimally invasive posterior cervical decompression using tubular retractor: the technical note and early clinical outcome. Surg Neurol Int 2014;5:34.

[8] Terai H, Suzuki A, Toyoda H, et al. Tandem keyhole foraminotomy in the treatment of cervical radiculopathy: retrospective review of 35 cases. J Orthop Surg Res 2014;9:38.

[9] Okazaki T, Nakagawa H, Mure H, et al. Microdiscectomy and foraminotomy in cervical spondylotic myelopathy and radiculopathy. Neurol Med Chir (Tokyo) 2018;58:468–76.

[10] Tanaka K, Mori N, Yokota Y, et al. MRI of the cervical nerve roots in the diagnosis of chronic inflammatory demyelinating polyradiculoneuropathy: a single-institution, retrospective case–control study. BMJ Open 2013;3:e003443.

[11] Tawa N, Rhoda A, Diener I. Accuracy of magnetic resonance imaging in detecting lumbo-sacral nerve root compromise: a systematic literature review. BMC Musculoskelet Disord 2016;17:386.

[12] Jinkins JR, Roeder MB. MRI of benign lumbosacral nerve root enhancement. Semin Ultrasound CT MR 1993;14:446–54.

[13] Georgy BA, Snow RD, Hesselink JR. MR imaging of spinal nerve roots: techniques, enhancement patterns, and imaging findings. Am J Roentgenol 1996;166:173–9.

[14] Rogosnitzky M, Branch S. Gadolinium-based contrast agent toxicity: a review of known and proposed mechanisms. Biometals 2016;29:365–76.

[15] Perazella MA. Gadolinium-contrast toxicity in patients with kidney disease: nephrotoxicity and nephrogenic systemic fibrosis. Curr Drug Saf 2008;3:67–75.

[16] Bao YF, Tang WJ, Zhu DQ, et al. Sensory neuronopathy involves the spinal cord and brachial plexus: a quantitative study employing multiple-echo data image combination (MEDIC) and turbo inversion recovery magnitude (TIRM). Neuroradiology 2013;55:41–8.

[17] Swami VG, Katlariwala M, Dhillon S, et al. Magnetic resonance imaging in patients with mechanical low back pain using a novel rapid-acquisition three-dimensional SPACE sequence at 1.5-T: a pilot study comparing lumbar stenosis assessment with routine two-dimensional magnetic resonance sequences. Can Assoc Radiol J 2016;67:368–78.

[18] Muhle C, Ahn JM, Biederer J, et al. MR imaging of the neural foramina of the cervical spine. Comparison of 3D-DESS and 3D-FISP sequences. Acta Radiol 2002;43:96–100.

[19] Vertinsky AT, Krasnokutsky MV, Augustin M, et al. Cutting-edge imaging of the spine. Neuroimaging Clin N Am 2007;17:117–36.

[20] Tins B, Cassar-Pullicino V, Haddaway M, et al. Three-dimensional sampling perfection with application-optimised contrasts using a different flip angle evolutions sequence for routine imaging of the spine: preliminary experience. Br J Radiol 2012;85:e480–9.

[21] Kaliya-Perumal AK, Ariputhiran-Tamilselvam SK, Luo CA, et al. Revalidating Pfirrmann's magnetic resonance image-based grading of lumbar nerve root compromise by calculating reliability among orthopaedic residents. Clin Orthop Surg 2018;10:210–5.

[22] Li Y, Fredrickson V, Resnick DK. How should we grade lumbar disc herniation and nerve root compression? A systematic review. Clin Orthop Relat Res 2015;473:1896–902.

[23] Hossein J, Fariborz F, Mehrnaz R, et al. Evaluation of diagnostic value and T2-weighted three-dimensional isotropic turbo spin-echo (3D-SPACE) image quality in comparison with T2-weighted two-dimensional turbo spin-echo (2D-TSE) sequences in lumbar spine MR imaging. Eur J Radiol Open 2019;6:36–41.

[24] Bodelle B, Luboldt W, Wichmann JL, et al. Chondral lesions in the patellofemoral joint in MRI: intra-individual comparison of short-tau inversion recovery sequence (STIR) with 2D multiple-echo data image combination sequence (MEDIC). Eur J Radiol Open 2016;3:259–63.

[25] Kohl S, Meier S, Ahmad SS, et al. Accuracy of cartilage-specific 3-Tesla 3D-DESS magnetic resonance imaging in the diagnosis of chondral lesions: comparison with knee arthroscopy. J Orthop Surg Res 2015;10:191.